



## UvA-DARE (Digital Academic Repository)

### Mechanics of filled rubbers from a molecular point of view

Varol, H.S.

**Publication date**

2017

**Document Version**

Other version

**License**

Other

[Link to publication](#)

**Citation for published version (APA):**

Varol, H. S. (2017). *Mechanics of filled rubbers from a molecular point of view*.

**General rights**

It is not permitted to download or to forward/distribute the text or part of it without the consent of the author(s) and/or copyright holder(s), other than for strictly personal, individual use, unless the work is under an open content license (like Creative Commons).

**Disclaimer/Complaints regulations**

If you believe that digital publication of certain material infringes any of your rights or (privacy) interests, please let the Library know, stating your reasons. In case of a legitimate complaint, the Library will make the material inaccessible and/or remove it from the website. Please Ask the Library: <https://uba.uva.nl/en/contact>, or a letter to: Library of the University of Amsterdam, Secretariat, Singel 425, 1012 WP Amsterdam, The Netherlands. You will be contacted as soon as possible.

## CHAPTER 6: FUTURE DIRECTIONS

Understanding the viscoelasticity of elastomer based nanocomposites is a very challenging task. Herein, I tried to see the nanocomposites during their linear and non-linear deformations from a molecular point of view. Even though the research presented here answer some crucial questions about mechanics of nanocomposites in terms of molecular structure of elastomers network during deformation and the effect of nanofiller dispersion, still many of questions about the magic behind viscoelasticity of nanocomposites remain unanswered. Limited variability in nanocomposite chemistry is one of the drawbacks of my project preventing me to find more universal answers to important questions. Next to increasing the variety of nanocomposites, also my methods which were used for explaining the reinforcement and strain-hardening of nanocomposites, should be applied for explaining different kind of deformation stages in nanocomposites, such as Payne effect, Mullins effect etc. Particularly my findings in Chapter 5 explaining strain-hardening characteristics in nanocomposites in monotonic (not repeating) stretching conditions must be reinforced by expanding the strain-hardening behavior of these samples in more real life use conditions, for instance, under cyclic deformations. Below, I will explain preliminary results of the strain-hardening behavior of NBR nanocomposites under cyclic forces.

### 6.1 Strain-hardening of nanocomposites under cyclic forces

During their production and practical uses, elastomer-based nanocomposites need to fulfill some important criteria, such as optimum processability, toughness, fatigue life etc., which have not been discussed in thesis. Among these factors, cyclability directly defines the life-time of some nanocomposites in practical applications. For instance, car tires during rolling undergo cyclic loading and the life-time of the tire tread under such deformation has been related to nano- to micro- size void transitions in the rubber.[199,200] In these studies, the dispersion of carbon black or other carbon allotropies (e.g., multi-wall carbon nanotube, MWCNT) has proven to have a positive effect on the life-time of the rubber under

## Future Directions

cyclic forces. This improvement is related to morphological changes of MWCNT fillers under cyclic deformations and the strong interaction between fillers and surrounding rubber matrix. Another recent study has elucidated the strain-hardening enhancement of material under cyclic loading due to the presence of uniformly dispersed  $\text{Fe}_3\text{O}_4$  nanofillers having physical cross-links with elastomer.[177] In the studied system, under cyclic stretching  $\text{Fe}_3\text{O}_4$  nanoparticles align along the direction of deformation and this alignment increases the total resistance of the composite to further deformations to the same direction. In our study, as mentioned before, there is no significant attraction between silica nanofillers and matrix, fillers are not perfectly dispersed and the strain hardening modulus changes due to filler amount is explained in terms of “bridging rubber” alignment to the stretching direction (see Chapter 5). However, as it is shown in Figure 6-1, under uniaxial stretching of an NBR nanocomposite ( $\Phi = 22.5$ ) sample at different cycles of stretching, we observed some interesting variations on the elasticity.

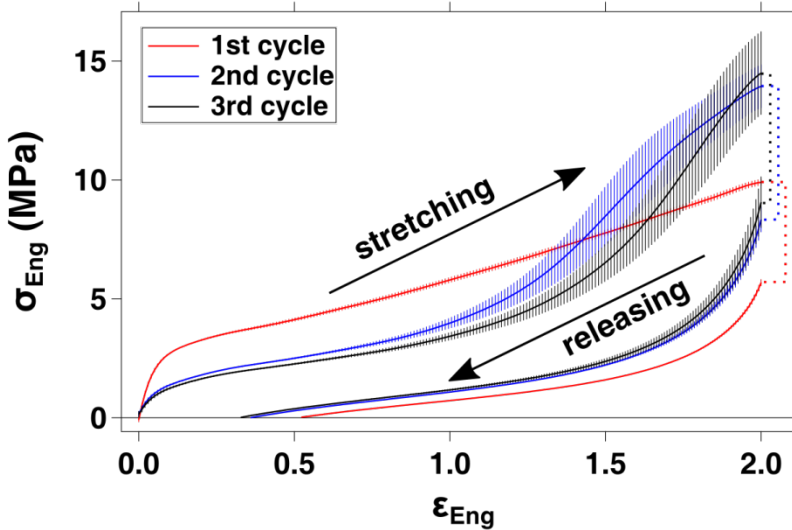


**Figure 6-1.** Engineering stress ( $\sigma_{\text{Eng}}$ ) – engineering strain ( $\epsilon_{\text{Eng}}$ ) characteristics under cyclic (3 cycles) loadings of  $\text{SiO}_2$  ( $\Phi=22.5$ ) / NBR nanocomposite. Curves under the arrow labelled as ‘releasing’ present  $\sigma_{\text{Eng}} - \epsilon_{\text{Eng}}$  curves of the sample during stress release till  $\sigma_{\text{Eng}}$  gets zero. Three curves between the two black arrows represent the  $\sigma_{\text{Eng}} - \epsilon_{\text{Eng}}$  behavior of the sample at each stretching from  $\epsilon_{\text{Eng}} = 0$  till  $\epsilon_{\text{Eng}} = 2$ . Error bars are standard deviation (SD) from 3 different dog-bone shape cut samples from the same nanocomposite slab.

For this experiment, I first cut three dog bone shape (length  $\approx 1$  cm, thickness  $\approx 0.2$  cm, width  $\approx 0.18$  cm) tensile test specimen from the slab of the highest volume filled NBR nanocomposite ( $\Phi = 22.5$ ). This sample is particularly interesting among all the other NBR systems (see Methods), since it has the most prominent strain-hardening characteristics at high strain levels in monotonic tensile tests discussed in Chapter 5. Each dog-bone shape sample is clamped (5 bar pressure) and stretched from  $\epsilon_{\text{Eng}} = 0$  till  $\epsilon_{\text{Eng}} = 2$  with the strain rate of 100 mm/min. During the cyclic mechanical tests, samples were held at  $\epsilon_{\text{Eng}} = 0$  and  $\epsilon_{\text{Eng}} = 2$  constantly for 2 minutes (dashed lines in Figure 6-1), in which we could stabilize the initial stress relaxation of the samples. Releasing (unstretching) the stress is carried out till the stress on the sample returns to zero ( $\sigma_{\text{Eng}} = 0$ ) with a constant strain rate of 50 mm/min. Before each stretching cycle, the initial stress level was tuned to zero by changing slightly the initial gap distance between clamps. First, second and third stretching cycles in the  $\sigma_{\text{Eng}} - \epsilon_{\text{Eng}}$  figure in Figure 6-1 are presented by using red, blue and black colors, respectively. In Figure 6-1, curves lies between the black arrows labelled as 'stretching' and 'releasing' present the  $\sigma_{\text{Eng}} - \epsilon_{\text{Eng}}$  curves of stretching at different cycles. The  $\sigma_{\text{Eng}} - \epsilon_{\text{Eng}}$  characteristics changing during unstretching (releasing) are shown under the black arrow labelled as 'releasing'.

In Figure 6-2a, the  $\sigma_{\text{True}} - \epsilon_{\text{True}}$  derived from  $\sigma_{\text{Eng}} - \epsilon_{\text{Eng}}$  stretching curves in Figure 6-1. Even without a quantitative analysis, it is apparent from the stretching curves from both  $\sigma_{\text{Eng}} - \epsilon_{\text{Eng}}$  and  $\sigma_{\text{True}} - \epsilon_{\text{True}}$ , that there is a clear effect of different cycles of stretching on the linear (initial slope of the curves at very low strain levels) and non-linear elasticity of the nanocomposite. Similar to previous studies aimed at obtaining the strain-hardening modulus,  $G_p$  at different number of cycles, [87,177,178,188] we also quantified  $G_p$  (see Chapter 5) of our sample with the help of linear fits to Gaussian plot at very high strains where there are almost linear correlations. Therefore, we did our linear fits to each slope in Figure 6-2b and (c) between  $\lambda^2 - (1/\lambda)$  values of 6 ( $\epsilon_{\text{True}} = 0.93$ ,  $\epsilon_{\text{Eng}} = 2.53$ ) and 8.66 ( $\epsilon_{\text{True}} = 1.1$ ,  $\epsilon_{\text{Eng}} = 3$ ) which is shown with a red box with dashed line in Figure 6-2b. The quantities of the slopes in each Gaussian curves (linear fits in Figure 6-2c) derived from different cyclic loadings is presented in Figure 6-2d. We have clearly observed that the strain-hardening modulus,  $G_p$  of the sample increases after each cycle of loading. On the top of this, this positive correlation between cycle of loading and  $G_p$  looks linear.

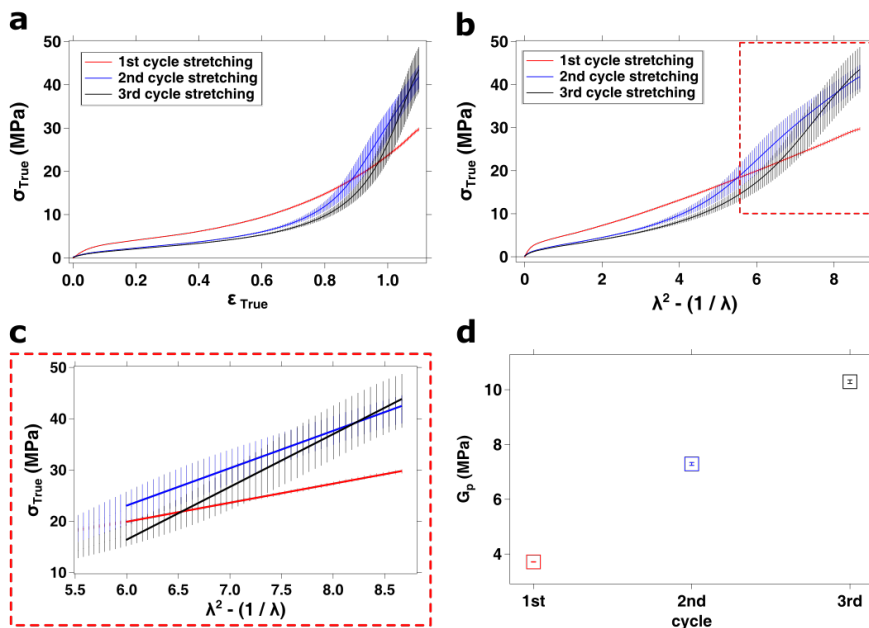


**Figure 6-2.** (a) True stress ( $\sigma_{\text{True}}$ ) – true strain ( $\epsilon_{\text{True}}$ ) curves of  $\text{SiO}_2$  ( $\Phi = 22.5$ ) / NBR nanocomposite at increasing number of stretching. (b) The Gaussian plots of the samples presented in (a). Red box sketched with dashed line represents the data range used for finding the slopes of each Gaussian curve at high strain levels. (c) Zoom in to the panel (b) is presented by showing the linear fits whose amplitude gives us the  $G_p$  presented in (d). Error bars are SD from three different dog-bone shape cut of the NBR system.

In the aforementioned literature, the “magic” behind the increase of  $G_p$  with increasing number of cycles has been explained in terms of inorganic filler alignment and enhanced interaction between fillers and surrounding rubber with each cycle.[177,178,188] In our systems, we do not have any significant chemical or physical interaction between filler and NBR and the morphology (shape) of fillers does not change with stretching (see Chapter 5). However, interestingly, in our systems we observe a clear hardening mechanism related to the number of loading cycles similar to the results on literature.

For the next steps of this preliminary work, we will repeat the cyclic mechanical tests for other NBR nanocomposites introduced in Chapter 5 and check their NBR chain anisotropy at each cycle. Performing the cyclic loading experiments of other nanocomposites will show us if this  $G_p$  and number of cycle relation is correlated also to the filler amount and/or filler size. And polarized Raman

## Chapter 6

experiments of the samples under cyclic forces might shed a light on the behavior of the “bridging chains” under cyclic deformations. One might naively guess that, previously mentioned delamination behavior of type -1 bound chains from filler surface and join to the type-3 (“bridging chains”) might be the key factor of obtaining higher  $G_p$  with increasing number of loading cycle. However, such hand-waving explanations must be validated in the near future by previously mentioned experiments to achieve a better understanding of the enhanced strain-hardening of the NBR nanocomposites with increasing numbers of stretching cycles.